Modelling the Presence of Diffuse Axonal Injury in Primary Phase Blast-Induced Traumatic Brain Injury

Matthew Sinclair, Adam Wittek, Barry Doyle, Karol Miller, Grand R. Joldes

Intelligent Systems for Medicine Laboratory, The University of Western Australia, Perth, Australia

Abstract

Blast induced traumatic brain injury (TBI) has been an affliction of war since the advent of militarised explosives and has become even more prominent with the resurgence of improvised explosive devices (IEDs). A common injury resulting from these blast events is Diffuse Axonal Injury (DAI), a clandestine type of TBI often occurring with no external visible symptoms. An voxel based finite element model of the human head allows for simulation of trauma mechanisms derived from hemispherical surface blast scenarios experimentally determined to have a greater than 99% survival rate by Bowen [1]. Coupling with *in vivo* results pertaining to DAI thresholds enabled introductory conclusions to be determined about the presence of DAI in survivable blast-trauma events. The blast events were simulated for the TNT mass equivalent of three different IEDs located at varying distances depending on the predicted survivability of the event. ABAQUS Explicit was used to conduct the finite element analysis and the Conventional Weapons (CONWEP) Blast Loading interface was used to calculate the hemispherical surface blast parameters. Areas of high strain occurred at the white/grey matter interface and brainstem for all simulations, as would be expected in a typical human head response. For the simulations in the lung-damage classification, there was insufficient strain to predict the presence of DAI. Conversely, most of the simulations from the 99% survivability distance produced sufficient strain to suggest DAI. Therefore, it was determined that blast events categorised as having a 99% survivability demonstrate sufficient strain to suggest at least mild DAI.

Keywords: Traumatic Brain Injury, Diffuse Axonal Injury, improvised explosive devices, voxel based finite element model

Introduction

Traumatic brain injury (TBI) has become one of the leading causes of death in the modern world [2] and impacts society medically, socioeconomically and emotionally [3]. Blast-Induced Traumatic Brain Injury (bTBI) has devastated military personnel since World War I, cloaked under the misclassification of shell shock, among other neurological disorders [4]. Recently, the necessity for understanding the nature of bTBI has become increasingly prevalent due to the insurgence of Improvised Explosive Devices (IEDs) in the Middle East conflicts. The precise mechanism of bTBI continues to evade the full comprehension of researchers due to the difficulty in obtaining accurate *in vivo* results via human experimentation. The nature and mechanisms that influence bTBI have been extrapolated from several animal-focused tests in combination with interpretation of computer-simulated models and finite element (FE) results. bTBI has become a key focus of military studies as the prominence of IEDs in modern combat continues to threaten the lives of war-fighters around the globe [5].

A primary objective of the investigative community is to determine numerical thresholds that allow for reasonable prediction of the injuries sustained by an individual due to either air or surface blasts. Through analysis of hemispherical surface blast events that are considered survivable on the Bowen survivability curve [1], an attempt at predicting the presence of diffuse axonal injury (DAI) under primary phase conditions can be established and will serve as a foundation for future research in methods of combating this devastating injury. The purpose of this study is to assess the prevalence of DAI in IED scenarios by simulating the effects of primary phase surface blasts using a voxel-based comprehensive computational model of the human head, and comparing the strain values within the brain to tested DAI strain injury criterion. Determination of the presence of DAI in these conditions will serve as a foundation for further study and has potential application within life-saving combat technology research.

Multiple investigations have been performed for air blast scenarios, but only few are accounting for the hemispherical blast surface events. Zhang et al. [6] investigated the influence of blast load dampening via a combat helmet, but only considered small explosives in close proximity to the head model, and only for air blast events. It was discovered that wearing an Advanced Combat Helmet may reduce strain by up to 30%, but these effects were not accounted for in this study. Explosive impacts on buildings from surface blasts have been studied in [7]. Wang [8] investigated air blast reflection for low mass explosives but primarily focused on bridging vein rupture. To the authors' knowledge, there has been no investigation into the hemispherical surface blast influences on producing DAI using an MRI-resolution head model.

Blast wave trauma has been categorised into four phases; influence from the overpressure waves; collision with shrapnel and flying debris; impact with surroundings from motion induced by blast force; and other factors such as chemical

burns or smoke inhalation. These are labelled as primary, secondary, tertiary and quaternary phases respectively [9]. Secondary and tertiary phases are typically compared to standard blunt-force induced TBI, whereas primary phase induced trauma is synonymous with explosive events. The precise mechanisms by which bTBI occurs are still unknown. Grujicic et al. [10] proposes that rotational motion and acceleration/deceleration are not applicable in blast-induced trauma scenarios. Conversely, an investigation by Dagro et al. [11] supports the notion that rotational loading is relevant to blast events. In addition, Elder [12] discovered injuries reminiscent of DAI by exposing live animals to blast pressure events, and attributes these injuries to rotational acceleration. Other injury mechanisms are hypothesised, including transmission of the pressure waves via vasculature [13].

Axonal damage, cerebral contusion, and subdural haemorrhaging are the three most common forms of mild TBI (mTBI), or concussion as it is known in common language [10]. Of these three forms of mTBI, DAI is the most difficult to detect by conventional means such as computed tomography (CT) scan or magnetic resonance imaging (MRI). DAI occurs when excessive stress or strain is applied to the directional axons within the white matter of the brain, usually resulting from accelerative and declarative forces caused by impact loads. Areas of particular susceptibility include the white/grey matter interface, the brainstem and areas around the falx cerebri. There is no agreement regarding the mechanical and tissue thresholds used for diagnosis of DAI in computational simulations. Experimental data produced by Bain et al. [14] by stretching tissue samples to the point at which predicted morphological injury occurred resulted in DAI threshold strain values ranging from 0.14 to 0.34, with an optimal value of 0.21. This was confirmed via FE analysis by Kleiven et al. [15] whom concluded that a max principle strain of 0.21 to 0.26 was indicative of DAI through a recreation of both NFL impact events and motorcycle accidents. Although many thresholds have been calculated via computational simulation, *in vitro* experimentation on human cadavers and human-resembling animal tissue samples remains as a strong basis for DAI threshold detection. For this reason, the empirical principle strain value of 0.21 was selected for use in this study. This threshold was applied to the results obtained from the FE simulation for multiple blast events to determine the presence of DAI.

Methods

Model and Material Properties

A finite element analysis was performed to determine the strains caused by blast loading within the brain, thereby requiring the use of a computational model of the human head. The model used was a 3D-voxel based mesh generated from an MRI

scanning of an anonymous human brain by Chen [16]. The FE mesh was constructed from hexahedral elements with approximate dimensions of 1.33 mm x 1.33 mm x 1.30 mm. The model consists of white and grey matter, cerebrospinal fluid (CSF) and skull, with material properties derived from Zhang [17]. Custom mesh smoothing algorithms were employed by Chen [16] to provide a better approximate shape of the anatomical features.

The falx cerebri and tentorium cerebellum are extensions of the dura fold separating the hemispheres of the brain and the cerebellum respectively. The original model provided by Chen [16] excluded these anatomical components. Their inclusion was deemed necessary in the simulations in an effort to improve the completeness of the model and to account for their effect on the system response to pressure waves. In addition, several studies empirically determined and reinforced the notions regarding the structural rigidity provided by the falx cerebri and tentorium cerebellum under cranial impacts: Smith et. al. [18] demonstrated that the falx cerebri provides high strains due to impairment of motion of the hemispheres and that the tentorium cerebellum can act as a physical obstruction over which axons can tear, subsequently leading to DAI. In addition, Zhang et al. [19] identifies the falx cerebri's strong effect on rotational loading and subsequently, the innocuous effect under translational loading. The falx cerebri and tentorium cerebelli were created by reassigning elements from the CSF, grey matter and white matter sets based on the geometry observed in coronal, sagittal and transverse MRI scans (Fig. 1). The maximum thickness was two elements (2.66mm) in the falx cerebri and three elements (3.99mm) in the tentorium cerebelli, with at least 4 nodes shared between membrane elements. The thickness used is essential in effectively transmitting bending forces under dynamic simulations and is hence modelled slightly thicker than the approximate membrane thickness of 2mm [20]. The increased thickness is taken into consideration by scaling the Young's modulus of the membranes in order to obtain the correct bending rigidity.

The properties for the introduced Falx Cerebri and Tentorium Cerebelli are taken from literature and listed in Table 1. All materials are modelled as linear elastic, except the white and grey matter, which are modelled as hyper-viscoelastic (Neo-Hookean with Prony series viscoelasticity).

Table 1. Material properties for Falx Cerebri and Tentorium Cerebelli

Tissue	Density ρ [kg/m^3]	Bulk modulus K [Pa]	Short term shear modulus G_0 [Pa]	Reference
Falx Cerebri	1130	4.47E+7*	4.62E+6*	[20]
Tentorium Cerebelli	1130	1.32E+7*	1.37E+6*	

* Scaled to account for difference in thickness

A fixed boundary condition was imposed at the stem of the head-spine juncture for this model. This boundary condition allows the introduction of rotational motion of the head, which is a key aspect of producing the strains hypothesised to in-

duce DAI. Chen [16] has analysed the effects of both the fixed and free boundary conditions via comparison with measurements published by Nahum et al [21]. He determined that the fixed boundary condition provides a reasonable approximation of the rotational acceleration undertaken by the head due to frontal impacts.

a) 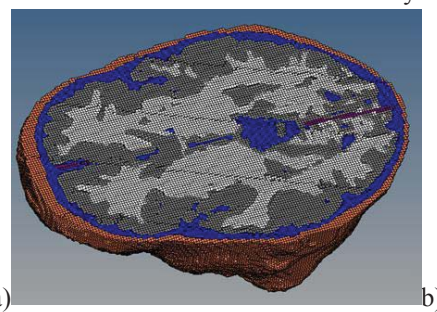 b) 

Fig. 1. a) Mid-transverse section of the head model. b) The introduced falx cerebri and tentorium cerebellum.

IED Simulation

ABAQUS Explicit was used for simulating the explosive events. Two methods of applying the blast loading are available in ABAQUS 6.13: interaction creation with manual amplitude input or use of the Conventional Weapons Effects in Blast Loading (CONWEP) system. The CONWEP system has been used, which calculates a reasonable blast wave inclusive of positive and negative impulses with the input of a TNT equivalence mass and impulse time. Also, the auto-calculation of reflection pressure is especially relevant in this analysis where hemispherical surface blasts are the primary blast loading mechanism.

The guerrilla nature of homemade IEDs makes them crude and variant in their constituents. A "typical" homemade IED is often constructed of 98% ammonium nitrate and 2% fuel oil [22]. In combat environments IEDs are usually made of either 105 mm or 155 mm artillery shells which cause more damage to vehicles and convoys, with the 155 mm shell being more explosive than the 105 mm [23]. Their explosive power is characterised by equating their mass specific energy to a TNT mass equivalence [22]. This is achieved through the multiplication of an empirically determined equivalency factor to determine a prediction for expected overpressure and impulse time of a non-TNT based explosion [24]. For ammonium-nitrate/fuel oil, 105 mm artillery shell, and 155 mm artillery shell, the TNT mass equivalents are 4.5, 2.4 and 7.3 kilograms respectively. This scaled comparison to an equivalent mass of TNT based on energy output allows for direct comparison between explosives of various constituents.

Using a combination of iterative equations derived by Kingery and Bulmash [25] and the Hopkinson-Cranz distance scaling equation (Eq. 1), the appropriate

standoff distance Z can be calculated to achieve the given blast parameters including blast overpressure and positive impulse time:

$$Z = \frac{R}{W^{1/3}} \quad (1)$$

where R is the actual distance between the detonation and contact points (m) and W is the TNT mass equivalence for the explosive (kg). Table 2 details these calculated values and the corresponding blast parameters. Values were chosen to be positioned on the lung damage threshold and 99% survivability curve [1]. These points were chosen as they demonstrate situations where people exposed to IED blasts would feel the impact, then presumably proceed with their duties without receiving medical attention. It is these scenarios that pose the greatest risk for patients induced with DAI as symptoms of concussions may exist but the full extent of the injury may be underestimated, possibly leading to death. It should be noted that no 2.4 kg explosion was analysed for the 99% survivability instance. This is because a standoff distance of 1.67m was required, thereby placing the detonation point above the ground. This reclassifies the explosion as an air blast and hence is not in the scope of this study.

Table 2. Simulated blast parameters calculated for IED scenarios

Survivability Curve	*TNT Mass Equivalent [Kg]*	*Standoff Distance [m]*	*Reflected Overpressure [kPa]*
Lung-damage	2.4	3.439	506.92
	4.5	4.123	549.20
	7.3	5.329	420.01
99%	4.5	2.340	2999.13
	7.3	3.413	1557.96

Results

The impact pressures, computed at the site of initial impact with the skull, for the various standoff distances and TNT mass equivalences are displayed in Figure 2. Consistent with the survivability curves and expected impacts, the impact pressures depended on the standoff distance and TNT mass equivalence, with the 4.5kg at 2.340m having the quickest and highest magnitude impact pressure and the 7.3kg at 5.329m conversely having the most delayed and smallest impact pressure. All pressure responses have jagged fluctuations, but the general gradients are similar to those predicted for the ideal Friedlander wave. This is most likely a result of intracranial pressures destructively and constructively interfering with the impact pressure as the results were probed from the impact site on the skull. The sites of impact also varied according to the distance of the

blast suggesting that ABAQUS Explicit has appropriately determined the pressure impact angles since the closer explosions impacted the head lower on the model. The 2.4kg explosion at 3.439m was the only impact pressure that developed a significant negative value, and then increased again above zero. This response was not as expected and could have been caused by a number of potential factors including the particular site of impact or an abnormality in the reflection of pressure waves within the head. Also, for all results, the pressure was analysed directly from the response of the skull, so an oscillating pattern is produced in the impact pressure. This is negligible since the main blast parameter of interest is the peak impact pressure induced.

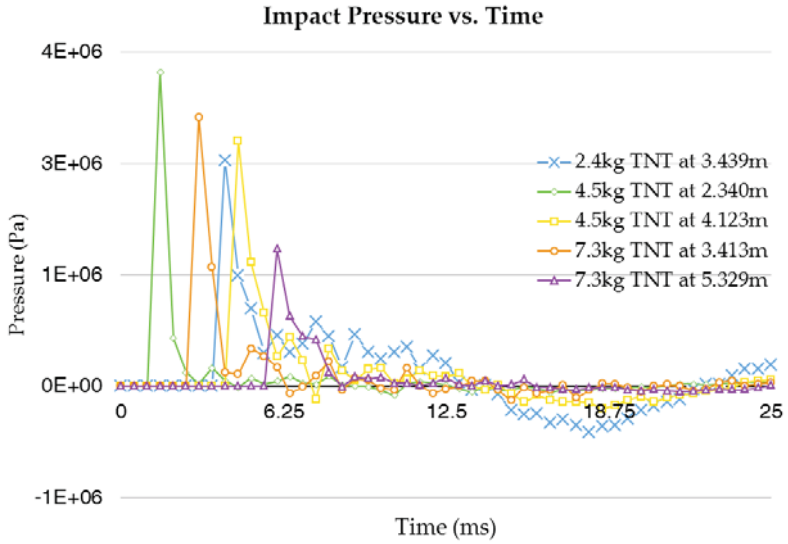

Fig. 2. Impact pressure acting on the skull for various TNT mass equivalencies and standoff distances.

For each of the blast events the response of the model was analysed to determine peak areas of strain (Figs. 3 and 4). It was noticed in all simulations that high regions of strain were present at the white/grey matter interface and the brainstem. This correlation demonstrates a realistic reaction from the model as one may see in head trauma events [26].

For the Lung Damage simulations the maximum strains were generally lower than the DAI threshold, indicating that DAI would generally not be induced by such explosions. For the 99% survivability simulations there is good indication that DAI will result from such events.

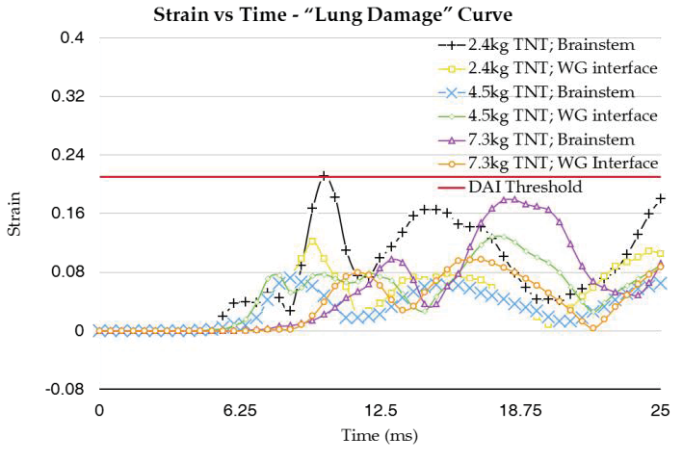

Fig. 3. The strain induced by explosions located on the Lung Damage iso-curve at areas of maximum principle strain in the brainstem and white/grey matter interface.

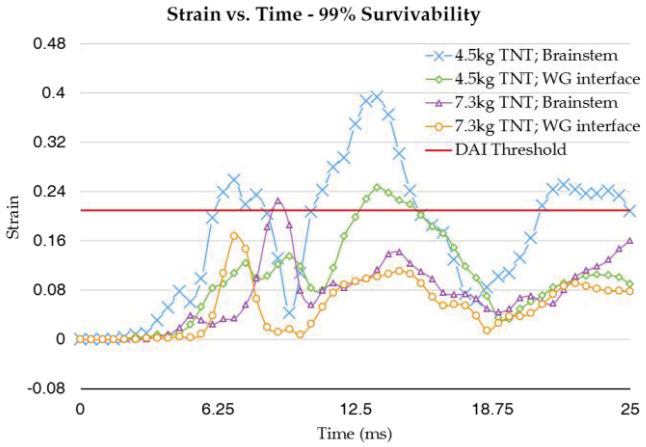

Fig. 4. The strain induced by explosions located on the 99% Survivability iso-curve at areas of maximum principle strain in the brainstem and white/grey matter interface.

Conclusions

Finite element simulations of different IEDs, for varying standoff distances according to the 99% survivability and lung damage iso-curves, were performed using the CONWEP surface hemispherical blast calculations in ABAQUS. The response of the brain was analysed and the principle strains compared to an experimental threshold 0.21 which was produced from empirical investigations for the presence of DAI. High regions of strain occurred at locations of the white/grey matter interface and brainstem for all simulations, both areas where DAI will typically be induced.

Strains lower than the threshold were computed for the lung damage curves, suggesting that DAI would not be present in these events. Significantly higher strains were computed for the 99% survivability events, strongly suggesting that at least mild DAI would be present in these events. This suggests such an analysis could be used for reasonable prediction of this injury in combat zones without the need for intrusive or expensive medical imaging.

Acknowledgments

The authors thank Prof. Martin Ostoja-Starzewski and Ms. Ying Chen from University of Illinois at Urbana-Champaign for providing the mesh of the head.

Bibliography

1. Bowen, I.G., E.R. Fletcher, and D.R. Richmond, *Estimate of man's tolerance to the direct effects of air blast.* 1968.
2. Monea, A.G., et al., *The biomechanical behaviour of the bridging vein-superior sagittal sinus complex with implications for the mechanopathology of acute subdural haematoma.* Journal of the Mechanical Behavior of Biomedical Materials, 2014. **32**: p. 155-165.
3. Topolovec-Vranic, J., et al., *Traumatic brain injury among men in an urban homeless shelter: observational study of rates and mechanisms of injury.* Canadian Medical Association Open Access Journal, 2014. **2**(2): p. E69-E76.
4. Hicks, R.R., et al., *Neurological effects of blast injury.* The Journal of trauma, 2010. **68**(5): p. 1257.
5. Kleinschmit, N.N., *A shock tube technique for blast wave simulation and studies of flow structure interactions in shock tube blast experiments.* 2011.
6. Zhang, L., R. Makwana, and S. Sharma, *Brain response to primary blast wave using validated finite element models of human head and advanced combat helmet.* Frontiers in neurology, 2013. **4**: p. 88.
7. Ngo, T., et al., *Blast loading and blast effects on structures—an overview.* Electronic Journal of Structural Engineering, 2007. **7**: p. 76-91.
8. Wang, C., *Finite Element Modeling of Blast-Induced Traumatic Brain Injury*, 2014, University of Pittsburgh.
9. Ling, G., et al., *Explosive blast neurotrauma.* Journal of neurotrauma, 2009. **26**(6): p. 815-825.
10. Grujicic, M., et al., *Fluid/Structure Interaction Computational Investigation of Blast-Wave Mitigation Efficacy of the Advanced Combat Helmet.* Journal of Materials Engineering and Performance, 2011. **20**(6): p. 877-893.
11. Dagro, A.M., et al., *A Preliminary Investigation of Traumatically Induced Axonal Injury in a Three-Dimensional (3-D) Finite Element*

Model (FEM) of the Human Head During Blast-Loading, 2013, DTIC Document.

12. Elder, G.A. and A. Cristian, *Blast-Related Mild Traumatic Brain Injury: Mechanisms of Injury and Impact on Clinical Care.* Mount Sinai Journal of Medicine, 2009. **76**(2): p. 111-118.
13. Bhattacharjee, Y., *Shell Shock Revisited: Solving the Puzzle of Blast Trauma.* Science, 2008. **319**(5862): p. 406-408.
14. Bain, A.C. and D.F. Meaney, *Tissue-level thresholds for axonal damage in an experimental model of central nervous system white matter injury.* Journal of biomechanical engineering, 2000. **122**(6): p. 615-622.
15. Kleiven, S., *Predictors for traumatic brain injuries evaluated through accident reconstructions*, 2007, SAE Technical Paper.
16. Chen, Y., *Biomechancial analysis of traumatic brain injury by MRI-based finite element modeling*, in *Mechanical Science & Engineering*2011, University of Illinois at Urbana-Champaign: Illinois, USA.
17. Zhang, L., K.H. Yang, and A.I. King, *A Proposed Injury Threshold for Mild Traumatic Brain Injury.* Journal of Biomechanical Engineering, 2004. **126**(2): p. 226-236.
18. Smith, D.H. and D.F. Meaney, *Axonal damage in traumatic brain injury.* The Neuroscientist, 2000. **6**(6): p. 483-495.
19. Zhang, J., et al., *Role of translational and rotational accelerations on brain strain in lateral head impact.* Biomed Sci Instrum, 2006. **42**: p. 501-506.
20. Yoganandan, N., *Frontiers in Head and Neck Trauma: Clinical and Biomechanical*1998: IOS Press.
21. Nahum, A.M., R. Smith, and C.C. Ward, *Intracranial pressure dynamics during head impact.* Proceedings of the 21st STAPP Car Crash Conference, 1977: p. 339-366.
22. Cormie, D., G. Mays, and P. Smith, *Blast effects on buildings*2009, London: Thomas Telford.
23. Panzer, M.B., et al., *Primary blast survival and injury risk assessment for repeated blast exposures.* Journal of trauma and acute care surgery, 2012. **72**(2): p. 454-466.
24. Díaz Alonso, F., et al., *Characteristic overpressure–impulse–distance curves for the detonation of explosives, pyrotechnics or unstable substances.* Journal of Loss Prevention in the Process Industries, 2006. **19**(6): p. 724-728.
25. Kingery, C.N., G. Bulmash, and U.S.A.B.R. Laboratory, *Air Blast Parameters from TNT Spherical Air Burst and Hemispherical Surface Burst* 1984: Ballistic Research Laboratories.
26. Liu, J., Z. Kou, and Y. Tian, *Diffuse axonal injury after traumatic cerebral microbleeds: an evaluation of imaging techniques.* Neural Regeneration Research, 2014. **9**(12): p. 1222.